

Hydrogen Gas Sensing with Networks of Ultrasmall Palladium Nanowires Formed on Filtration Membranes

X. Q. Zeng,^{†,‡} M. L. Latimer,^{†,§} Z. L. Xiao,^{*,†,§} S. Panuganti,[§] U. Welp,[†] W. K. Kwok,[†] and T. Xu[†]

[†] Materials Science Division, Argonne National Laboratory, Argonne, Illinois 60439, United States and [‡] Department of Chemistry and Biochemistry and [§] Department of Physics, Northern Illinois University, DeKalb, Illinois 60115, United States

ABSTRACT Hydrogen sensors based on single Pd nanowires show promising results in speed, sensitivity, and ultralow power consumption. The utilization of single Pd nanowires, however, face challenges in nanofabrication, manipulation, and achieving ultrasmall transverse dimensions. We report on hydrogen sensors that take advantage of single palladium nanowires in high speed and sensitivity and that can be fabricated conveniently. The sensors are based on networks of ultrasmall (<10 nm) palladium nanowires deposited onto commercially available filtration membranes. We investigated the sensitivities and response times of these sensors as a function of the thickness of the nanowires and also compared them with a continuous reference film. The superior performance of the ultrasmall Pd nanowire network based sensors demonstrates the novelty of our fabrication approach, which can be directly applied to palladium alloy and other hydrogen sensing materials.

KEYWORDS Hydrogen sensor, palladium, nanowires, networks

Hydrogen (H_2) gas is considered to be one of the most promising clean energy carriers for use in fuel cells and combustion engines.¹ It is also used extensively in scientific research and industry, notably in glass and steel manufacturing as well as in the refining of petroleum products.² Effective H_2 sensors that can quickly and sensitively respond to H_2 gas are crucial for the safe deployment of all hydrogen-based applications. Large scale industrial sensing has been achieved using gas chromatography or mass spectrometry systems. The bulky and expensive equipment required by these systems, however, makes them unsuitable for many applications.^{2,3} Other commercially available H_2 sensors, even those designated for fuel cell applications, have drawbacks on size and response time.⁴ Ideally, a H_2 gas sensor should be compact, sensitive, and durable, have short response times, and be simple to fabricate.²

Materials that change their resistivity in the presence of H_2 are among the most attractive for sensors due to their compact packaging and relatively straightforward signal readout.^{5–7} In the presence of H_2 the resistance of Pd will change due to the formation of a solid solution of Pd/ H (at low H_2 pressure, α -phase) or a hydride (at high H_2 pressure, β -phase).⁸ Furthermore, Pd is highly selective to H_2 , enabling Pd to be an excellent H_2 sensing material. In fact, most of the room-temperature solid-state H_2 sensors in a chemically

variable environment use Pd metal and alloys as sensing elements.^{7–12}

Several fundamental problems are associated with bulk Pd-based hydrogen sensors. First, the diffusion of the hydrogen into bulk Pd such as a thick Pd film can result in an extraordinary large internal stress, leading to buckling of the films.^{13,14} This irreversible deformation leads to an irreversible resistance change, hence eliminating reusability. Second, the hydrogen atom diffusion in Pd is very slow at room temperature (the diffusion coefficient is $3.8 \times 10^{-7} \text{ cm}^2/\text{s}$ at 298 K).¹⁵ Thus, the long diffusion pathway of hydrogen into bulk Pd structures inevitably results in a long response time.

Progress in nanoresearch has led to the development of H_2 sensors based on Pd nanomaterials.^{15–24} Among them, sensors based on single Pd nanowires^{8,15,18,19,23,24} showed promising results in speed, sensitivity, and ultralow power consumption. The utilization of individual Pd nanowires as sensing elements, however, can face challenges in nanofabrication, manipulation, and achieving small transverse dimensions that are essential to the speed and sensitivity of the sensors. Scientists have developed/utilized various approaches to fabricate single Pd nanowires: (1) electrodepositing Pd at the step-edges on graphite,^{16,17} (2) electrodepositing Pd into nanochannels of porous membranes, e.g., anodic aluminum oxide,¹⁸ (3) lithographically patterned nanowire electrodeposition (LPNE)²⁵ of Pd on sacrificial nanoelectrodes predefined on an insulating substrate,^{15,23,24} and (4) patterning Pd films via electron-beam (e-beam) lithography¹⁹ or deposition and etching under angles (DEA) methods.⁸ The last two approaches need nano- (e.g., e-beam

* To whom correspondence should be addressed, xiao@anl.gov or zxiao@niu.edu.

Received for review: 10/20/2010

Published on Web: 00/00/0000

lithography tool) or microfabrication machines and multiple lithography processes. In the first approach, it will be inconvenient to reproducibly and massively fabricate single Pd nanowires by electrodepositing them on step-edges of graphite substrates. Furthermore, the nanowires grown on conducting graphite need to be relocated to an insulating substrate. Electrodepositing Pd into nanochannels of porous membranes is a convenient way to obtain large quantities of Pd nanowires. However, the problem is to make electrical contacts to individual nanowires which typically requires the use of photo- or e-beam lithography and subsequent film deposition, resulting in a tedious fabrication process. Moreover, the surfaces of these nanowires can be contaminated during the process of dissolving the porous membranes to release the nanowires, degrading their gas-sensing performance.

Here, we present a new fabrication approach that takes advantages of single palladium nanowires for hydrogen sensing while eliminating their nanofabrication obstacles. The sensors are based on networks of ultrasmall palladium nanowires achieved by depositing palladium onto commercially available filtration membranes. The transverse dimensions (thickness and width) of the palladium nanowires are less than 10 nm. The response times of the Pd nanowire networks decrease with shrinking transverse dimensions and are much shorter than those of reference continuous films of the same thickness.

Porous Anodisc inorganic membranes from Whatman have been widely used as filters in chemistry. The straight nanochannels in the bulk of the membranes have also been utilized as templates to grow nanowires^{18,26,27} and nanotubes.²⁰ Though the available nominal effective filtration pore diameters are 20, 50, 100, and 200 nm, on the surface, the diameter of the nanochannels in the bulk of the membrane is unchanged (i.e., 200 nm).²⁷ The effective filtration of the membranes with pore diameter smaller than 200 nm is determined by the pore diameters of a very thin (~300–400 nm) layer of a nanoporous network array supported on top of a 60 μ m thick membrane containing vertical nanochannels 200 nm in diameter, as shown by the cross-section micrograph given in inset of Figure 1a. For a nominal effective filtration pore diameter of 20 nm, the material sections between neighboring pores is less than 10 nm wide (please see Figure 4b in ref 27 for a micrograph on the surface of a bare membrane). We utilized these sections as a template to form a wire network array of Pd by depositing Pd onto it.

Anodisc 13 membranes with a nominal filtration pore diameter of 20 nm were purchased from Whatman Company.²³ They were cleaned with acetone in a ultrasonic bath for 10 min and rinsed with deionized water followed by ethanol and dried with high-purity nitrogen gas. With the filtration layer facing the Pd target, we sputtered Pd onto the filter surface of the membrane using an ATC-2400 thin film deposition system with a base vacuum of $\sim 1 \times 10^{-7}$ Torr. Argon was used as the working gas at a pressure of 3 mTorr.

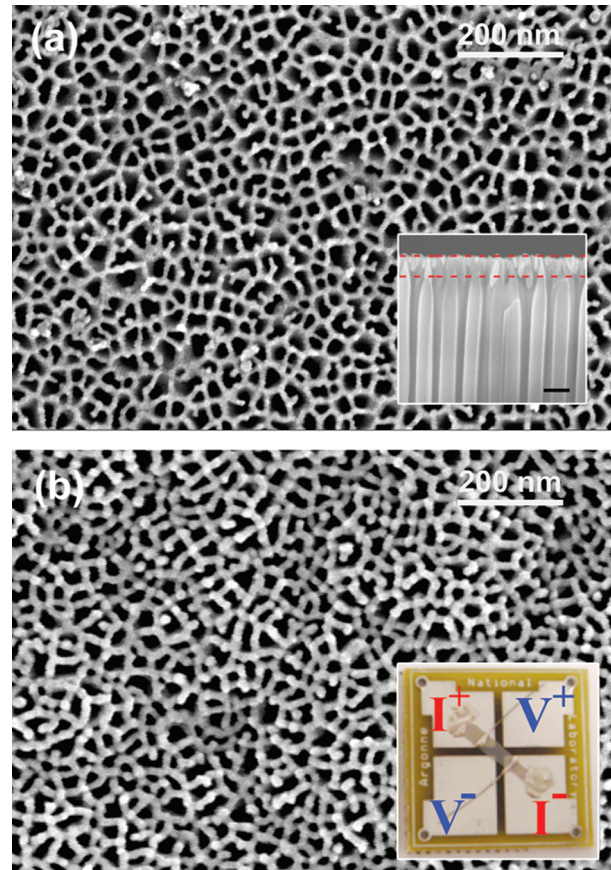


FIGURE 1. Scanning electron microscopy (SEM) micrographs of networks of Pd nanowires. The nominal thickness of the deposited Pd is 7 nm (a) and 30 nm (b), respectively. Inset to (a) is a cross-section SEM micrograph of an Anodisc 13 membrane with filtration pore diameter of 20 nm. The part between the two red dashed lines is the effective filtration layer. The black scale bar in the inset is 400 nm. Inset to (b) presents an optical image of a sample cut out from the Pd-coated membrane mounted on a sample holder.

A deposition rate of 1.3 Å/s determined by an in situ quartz crystal microbalance (QCM) thickness monitor (model TM-350 from Maxtek, Inc.) was used to calculate the sputtering time for a desired nominal thickness of the deposited Pd. The final products were imaged with a high-resolution field emission scanning electron microscope (SEM) (Hitachi S-4700 II). A rectangle-shaped sample was cut out from the Pd-coated membrane and mounted onto a sample holder with four silver pads. Electrical connections were made from the silver pads to a current source (Keithly 6221) and to a digital to analog (DAC) board (NI6259) via a voltage preamplifier (SR560). Silver paste was used to attach the wires to the silver pads. Standard four-contact resistive measurements were carried out at a constant current mode with current ranging from tens of nanoamperes to a few milliamperes, depending on the sample resistance. The inset to Figure 1b shows an optical image of the device with the Pd-coated side facing up. A homemade hydrogen sensor testing system using a series of ultrafast solenoid valves and a minimized dead volume of the gas passages was used to accurately

characterize these sensors with response times down to tens of milliseconds.²¹ H₂ gas (Airgas, ultrahigh purity) was premixed with N₂ gas (Airgas, ultrahigh purity) to a desired concentration using flow controllers (Aalborg GFC17A). We replaced the pure H₂ with certified 1 % or 0.1 % H₂ balanced in N₂ to achieve H₂ concentration at parts per million levels. N₂ was also used as the purging gas. The total gas flow rate was 200 sccm. All the tests were conducted at room temperature.

Figure 1 presents top-view SEM micrographs of Anodisc 13 membranes with pore diameter of 20 nm after deposited Pd with nominal thicknesses of 7 and 30 nm, respectively. By comparing Figure 1a to Figure 4b in ref 27, one finds that the morphology of the membrane does not change significantly after coating with 7 nm thick Pd. With increasing thickness of the deposited Pd, however, the pores shrink and the widths of the Pd sections between neighboring pores become larger, as can be seen from the micrograph presented in Figure 1b. Quantitatively, the widths of the Pd nanowires (i.e., sections between the pores) in panels a and b of Figure 1 are 7–9 and 12–15 nm, respectively. Though we did not carry out detailed investigations on the relationship between the width of the Pd nanowires and the nominal thickness of the deposited Pd, it is reasonable to estimate that their widths are close to the widths of the sections between pores in the bare templates and their thickness is that of the deposited Pd if its nominal thickness is less than 10 nm. This relation is more complicated with thicker deposited Pd. We find that wire networks with deposited Pd less than 10 nm are more promising as sensors. Those with thicker deposited Pd were also studied for comparison.

A plot of the time dependence of the resistance for a 7 nm thick Pd nanowire network at various H₂ concentrations is shown in Figure 2. In the presence of hydrogen gas the resistance of the sample increases with time and saturates at a value that depends on the gas concentration. The inset to Figure 2 demonstrates the concentration dependence of the maximal resistance change $\Delta R_M/R_0$ and the response time which is defined as the rise time to reach 90 % of its maximal change. The results are similar to those reported for electrodeposited nanowires¹⁵ where $\Delta R_M/R_0$ first increases with H₂ concentration up to about 3 % and then remains constant at higher concentrations. Furthermore, quantitative analysis demonstrates that the concentration dependence of the maximal resistance change follows a power-law relation with an exponent of 0.58 for concentrations up to 3 %. This indicates that the interaction of H₂ and Pd in this concentration range follows Sievert's law.²⁸ That is, the ratio of the dissolved atomic hydrogen to Pd atoms can be described to a good approximation with a power-law dependence of the hydrogen partial pressure (i.e., H₂ gas concentrations in our experiments) and the change of this ratio leads to a proportional $\Delta R_M/R_0$ response.²⁸ The exponent of 0.58 is slightly larger than those ($\sim 0.4\text{--}0.50$) reported in the literature for Pd films.^{14,28} However, as

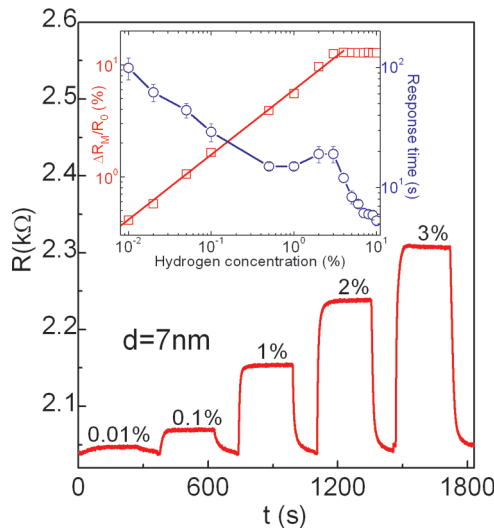


FIGURE 2. H₂ response to a 7 nm thick Pd nanowire network. Inset: H₂ concentration dependences of the maximal resistance change $\Delta R_M/R_0$ and response time. R_0 is the resistance in the absence of hydrogen gas and ΔR is defined as the absolute resistance change $R(t) - R_0$ and ΔR_M is the maximal resistance change at a specific concentration. The response time is defined as the rise time to reach 90 % of its maximal change, i.e., $\Delta R/\Delta R_M = 0.9$. The solid line is a power-law fit with an exponent of 0.58.

shown in Figure 3a, the exponent decreases when the transverse dimensions (thickness, width, or both) of the Pd nanowires are increased. For example, we obtain an exponent of 0.46 for the 30 nm thick Pd nanowire network. Since a larger power-law exponent corresponds to a faster change in resistance with changing H₂ concentration, this implies that sensors with smaller transverse dimensions have better sensitivity. This is reasonable because the surface to volume ratio will be larger in Pd nanowires with smaller transverse dimensions and the surface can have denser atomic hydrogen sites than the bulk.¹⁸

The $\Delta R_M/R_0$ saturation at a H₂ concentration of 3 % is related to the transition from α -phase to β -phase of the Pd/H system. The resistance of the β -phase is not sensitive to the change in H₂ concentration. This transition has also significant effect on the response time. As presented in the inset of Figure 2 for the 7 nm thick Pd nanowire network, the response time at low H₂ concentrations becomes shorter when more H₂ is present. However, the sample needs longer time to reach its steady state at H₂ concentrations of 1–3 % than that at 0.5 %, resulting in a bump in the response time versus concentration curve. Both the response time and its concentration dependence are quantitatively comparable to those of the smallest electrodeposited single Pd nanowire (please see Figure 7e in ref 15) where the small bump was attributed to the α -to β -phase transition. This bump evolves into a peak with increasing transverse dimensions, as shown in Figure 3b for the Pd nanowire networks with nominal thicknesses of 17 and 30 nm for the deposited Pd. As expected, Figure 3b also shows that the response time

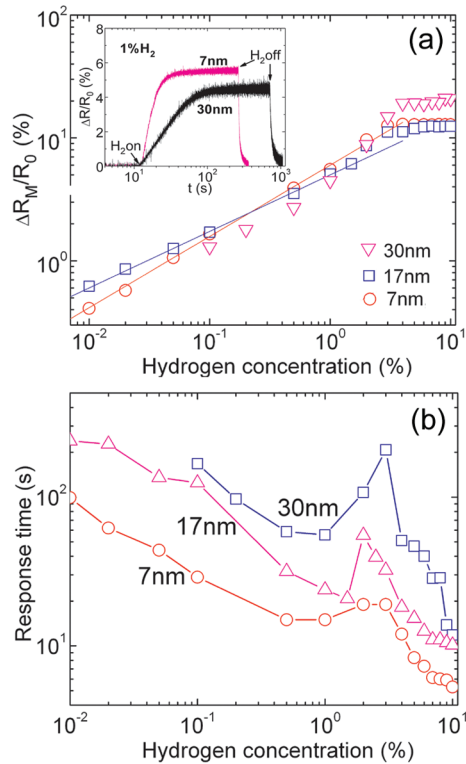


FIGURE 3. Comparisons of the hydrogen responses of Pd nanowire networks with various nominal thicknesses of the deposited Pd: (a) and (b) present H₂ concentration dependences of the resistance changes $\Delta R/R_0$ and response times, respectively. The solid lines to fit the data of the 7 and 30 nm thick Pd nanowire networks represent power-law exponents of 0.58 and 0.46, respectively.

becomes longer at all H₂ concentrations for samples with thicker Pd nanowires.

Lee et al.¹⁸ found that the buckling and hysteresis behaviors observed in thick ($d > 20$ nm) Pd films do not appear in continuous ultrathin films ($d = 5$ nm). Since the thickness of a few nanometers is so small, one might think the response time of such an ultrathin Pd film to H₂ gas could be very short and it might be close to that of an ultrathin nanowire. If this were the case, H₂ sensors based on ultrathin Pd films would be preferable since it is more convenient to fabricate ultrathin films than ultrathin nanowires. Thus, it is necessary to compare the H₂ responses of ultrathin Pd films and our network of ultrathin Pd nanowires. In our experiments, a Si substrate (with a SiO₂ layer of 100 nm thick) was placed near the Anodisc 13 membrane and Pd was deposited onto them simultaneously, ensuring the same thickness for both the Si substrate reference film sample and the Anodisc substrate sample. Figure 4a presents the evolution of the resistance change for the 7 nm thick network of Pd nanowires and its reference film at H₂ concentrations of 0.1 % and 1 %. It is evident that the reference film requires a much longer time to reach its steady state. As shown in Figure 4b and in its inset, for the 7 and 12 nm thick samples, the response times of the reference films were almost 1 order of magnitude longer than those of the nanowire

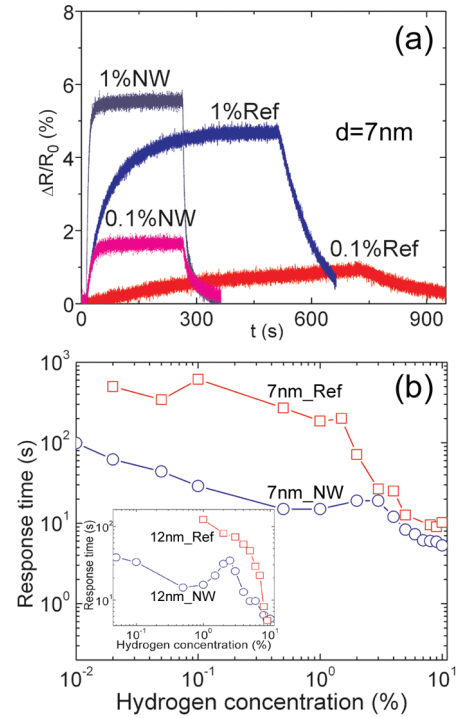


FIGURE 4. Comparisons of the hydrogen responses of Pd nanowire networks (NW) and their reference films (Ref): (a) resistance changes $\Delta R/R_0$ with time at H₂ concentrations of 0.1 % and 1 %; (b) concentration dependences of the response times. The nominal thicknesses of the deposited Pd are given in the figures.

networks at H₂ concentrations below 1 %, though the difference becomes smaller at high H₂ concentrations, i.e., in the β -phase. The results clearly demonstrate that for a Pd object with dimensions down to a few nanometers, H₂ diffusion from the sides or, as discussed later, the surface to volume ratio plays a critical role in the H₂ response time.

The above results directly imply that networks of Pd nanowires with even smaller transverse dimensions should be pursued. Since the width of the Pd nanowires is close to that of the template (the width of the sections between neighboring pores in the Anodisc 13 membrane) which is fixed, we reduced their thickness by depositing less Pd. Experimentally we examined samples with Pd thickness down to 2 nm with a thickness interval of 0.5 nm. The samples with thickness less than 3.5 nm have resistance (>100 M Ω) over the input impedance of our electronic circuit. A typical time dependence of the resistance for a 4 nm thick network of Pd nanowires in the presence of hydrogen gas is presented in Figure 5a. Differing from the data shown in Figures 2, 3a, and 4a, this sample became more conductive upon H₂ exposure. This behavior is very similar to that observed in fractured single Pd nanowires where the decrease of resistance is attributed to the disappearance of gaps due to the dilation of the Pd after absorbing hydrogen.^{15,16} This means that when the thickness of the coated Pd layer is extremely thin (e.g., 4 nm), the Pd nanowires forming the network become discontinuous. As shown by the concentration dependence of the resistance

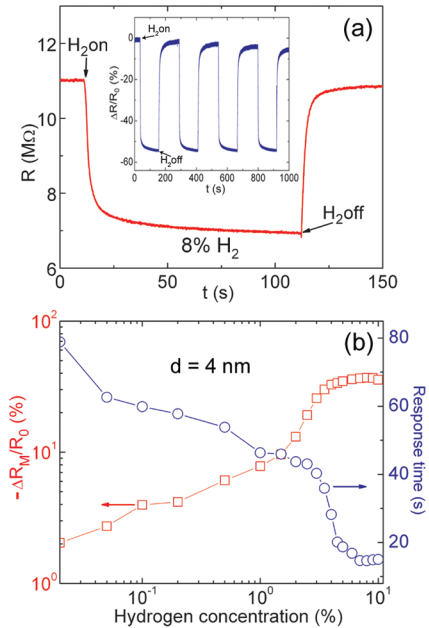


FIGURE 5. H_2 response of a 4 nm thick Pd nanowire network: (a) resistance change $\Delta R/R_0$ with time at H_2 concentration of 8%. Inset shows data with more cycles for a sample made from different parts of the same membrane. (b) Concentration dependences of the maximal resistance change $\Delta R_M/R_0$ and response time.

change $\Delta R_M/R_0$ presented in Figure 5b, however, our sample can detect hydrogen at concentration levels down to 0.01 % while the resistance of the fractured electrodeposited Pd nanowires¹⁵ changes only at a H_2 concentration of 1 % or higher. This difference can be understood in terms of physical gap sizes: the gaps in electrodeposited nanowires are tens of nanometers or larger. The significant volume increase of the β -phase that occurs at H_2 concentrations of 1 % or higher is needed to make them closed. On the other hand, the gaps in our sample are very small and electrons can tunnel through them. Any slight volume change due to the hydrogen-induced palladium lattice expansion can make the gap smaller, leading to better electron tunneling and hence to a resistance decrease. In fact, both the capability to detect H_2 at low concentrations and the resistance change $\Delta R/R_0$ of this 4 nm thick network of Pd nanowires are comparable to those of the two-dimensional (2D) Pd nanocluster array formed on a glass substrate covered with a self-assembled monolayer (SAM).²¹ The latter has gaps of a few nanometers between neighboring nanoclusters and electron tunneling dominates the electric properties at low H_2 concentrations. As shown by the response times at various H_2 concentrations given in Figure 5b, however, the 4 nm thick network of Pd nanowires is much slower than the SAM promoted 2D Pd nanocluster array in response to H_2 exposure. This highlights the importance of SAM induced reduction of the stiction between the palladium and the substrate to the response time of the sensor. The strong adhesion of Pd on the substrate may also prevent some of the Pd atoms to return to their original locations, resulting in an decrease

of the amplitude of the resistance change with increasing cycles as that shown in the inset of Figure 5a. Though siloxane was successfully used to achieve SAMs on glass substrates, efforts are needed to find appropriate molecules to form SAMs on the Anodisc filtration membranes.

Theoretically, one gap in a single nanowire causes it to be discontinuous and nonconductive. For a network of nanowires, however, gaps in some of the nanowires can only increase the resistance of the network rather than make it nonconductive because electrons can always flow through the conducting pathways as long as the number of the broken nanowires is below the percolation threshold. This implies that the transition or a crossover from a network without a significant number of broken nanowires to that consisting of mainly broken nanowires should be second order. The data in Figure 2 show that the number of broken Pd nanowires in the 7 nm thick network is negligible and that its H_2 sensing mechanism is based on the resistance change of the nanowires upon H_2 exposure. Meanwhile Figure 5 indicates that broken Pd nanowires dominate the electric transport of the 4 nm thick network and its H_2 sensing mechanism is based on a resistance decrease due to the H_2 induced closure of gaps. Networks with thicknesses between 4 and 7 nm may have a large number of broken Pd nanowires while there are also many flow pathways for electrons through continuous nanowires. That is, the mentioned two sensing mechanisms may compete in some networks where the thicknesses range from 4 to 7 nm. In fact, such a behavior does occur in a 4.5 nm thick network. As presented in Figure 6a, the resistance versus time curves for H_2 concentrations of 20 % and 50 % have two peaks just after the H_2 is turned on and off. The first peak corresponds to the fast resistance increase from the through pathways of continuous Pd nanowires upon H_2 exposure, followed by the closure of gaps in the broken nanowires which leads to an opposite resistance decrease. On the other hand, the resistance increase at the second peak when H_2 is turned off is due to the gap reopening in the previous broken nanowires while the decay is due to the release of H_2 from the continuous Pd nanowires. Figure 6a also indicates that high H_2 concentrations are needed to observe both of the sensing mechanisms in the same sample. This is because newly formed electron flow pathways from the broken nanowires due to the H_2 induced gap closure are in parallel to those of the existing continuous nanowires. Furthermore, there are gaps of various sizes in broken nanowires and one gap can destroy an electron flow pathway. Higher H_2 concentration can induce larger expansion of the Pd lattice thus decreasing the density of gaps so that more new flow pathways can be formed. At low H_2 concentration, the resistance change induced by the gap-closure in some broken nanowires cannot change the total resistance significantly. Thus the sample can reach a steady state, as shown by the curve obtained at H_2 concentration of 3 %. By comparing the responses of the 7 and 4.5 nm networks to

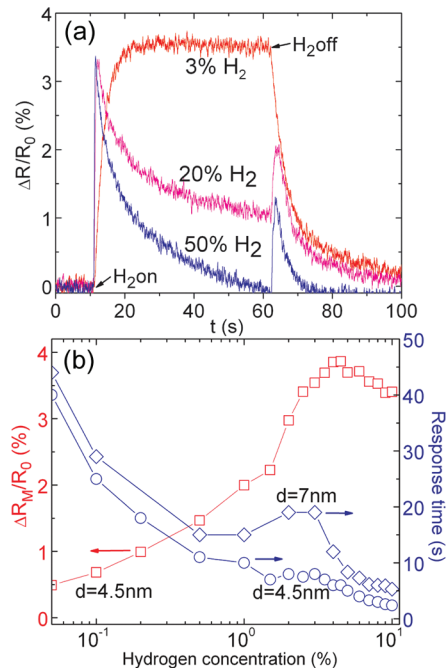


FIGURE 6. H₂ response of a 4.5 nm thick Pd nanowire network: (a) resistance changes $\Delta R/R_0$ with time at various concentrations. (b) Concentration dependences of the maximal resistance change $\Delta R_m/R_0$ and response time. The response times of the 7 nm thick sample at various concentrations were also replotted in (b) for comparison.

3 % H₂ as given in Figure 2 and Figure 6a, we found that the resistance change $\Delta R_m/R_0$ in the latter is a factor of ~ 4 smaller. In fact, as shown in Figure 6b the $\Delta R_m/R_0$ of the 4.5 nm thick network are smaller than those of the 7 nm thick one at all the measured H₂ concentrations. This is simply because the latter has more parallel through-pathways of the continuous nanowires that contribute to the total resistance change upon H₂ exposure.

H₂ response times of the 4.5 nm thick network at various concentrations are presented in Figure 6b. They are indeed shorter than those of the 7 nm thick sample at all tested H₂ concentrations. However, the shortening of the response time with decreasing thickness from 7 to 4.5 nm is more significant at H₂ concentrations higher than 1 %. As experimentally revealed by Fang et al.,²⁴ H₂ response of a small Pd nanowire is limited by the surface reaction, i.e., the surface area to volume ratio rather than proton diffusion. In fact, our data at H₂ concentrations less than 1 % are consistent with their findings: the slightly shorter response times observed in the 4.5 nm thick sample can be understood considering the surface area to volume ratio increase of ~ 1.2 instead of the change of a factor of ~ 2.4 in diffusion time estimated with Einstein's expression $x = \sqrt{2Dt}$, where x , D , and t are the length, coefficient, and time of the diffusion.²⁴ The additional improvement in response times of the 4.5 nm network at H₂ concentration higher than 1 % is apparently due to the disappearance of the retarding response times at H₂ concentrations of 2–3 % observed in the thicker

sample. Since the retarding response times are associated with the α to β phase transition and occur in the coexistence region of $\alpha + \beta$ phases, the monotonic decrease of the response time with increasing H₂ concentration in the 4.5 nm thick sample implies a suppression or disappearance of the $\alpha + \beta$ phases coexistence region. In fact, systematic X-ray diffraction (XRD) investigations on both Pd nanoparticles²⁹ and nanocrystalline Pd³⁰ did reveal narrowing of the $\alpha + \beta$ phases coexistence region with decreasing particle or grain size. It was found that this size effect is due to the downshift in the critical temperature T_c for the phase boundary of the coexistence region.^{29,30} That is, the effect of decreasing the particle/grain size on the $\alpha + \beta$ phases coexistence region is similar to that induced by increasing temperature. This is indeed consistent with the disappearance of retarding response times in heated Pd nanowires.²³

Similar to that observed in single pure Pd nanowires¹⁵ and thin films,^{2,14,21} the resistance change $\Delta R_m/R_0$ of our networks of Pd nanowires saturates at H₂ concentrations higher than 3 %. This can seriously hinder the applications of sensors based on such networks. As demonstrated by the disappearance of the $\Delta R_m/R_0$ saturation in the H₂ response of Pd/Ni alloy films;^{28,31} however, such a limitation in our Pd nanowire networks could be eliminated by replacing the pure Pd with Pd alloys. In fact, we chose pure Pd to fabricate the networks simply because data on single Pd nanowires are available for comparison.

In summary, we achieved a new type of hydrogen sensor based on networks of ultrasmall (<10 nm) palladium nanowires formed on commercially available filtration membranes. The sensors have high sensitivity and short response times. Our approach can also provide a general way to utilize the improved performance or new properties of single nanowires of Pd alloy and other hydrogen-sensing materials while eliminating the nano-fabrication obstacles.

Acknowledgment. The work on nanowire fabrication was supported by the Department of Energy (DOE) Grant DE-FG02-06ER46334. X.Q.Z. acknowledges partial support by the Nanoscience Fellowship of Northern Illinois University. We are grateful to Michael P. Zach and Phillip Stone for their technical assistance. The thin film deposition and morphological analyses were performed at the Center for Nanoscale Materials (CNM) and Electron Microscopy Center (EMC) of Argonne National Laboratory which is funded by DOE BES under Contract No. DE-AC02-06CH11357.

REFERENCES AND NOTES

- (1) Crabtree, G. W.; Dresselhaus, M. S.; Buchanan, M. V. *Phys. Today* **2004**, *57*, 39.
- (2) Ramanathan, M.; Skudlarek, G.; Wang, H. H.; Darling, S. B. *Nanotechnology* **2010**, *21*, 125501.
- (3) Liekus, K. J.; Zlochower, I. A.; Cashdollar, K. L.; Djordjevic, S. M.; Loehr, C. A. *J. Loss Prev. Process Ind.* **2000**, *13*, 377.
- (4) <http://www.fuelcellsensor.com/>.
- (5) Tibuzzi, A.; Di Natale, C.; D'Amico, A.; Margesin, B.; Brida, S.; Zen, M.; Soncini, G. *Sens. Actuators, B* **2002**, *83*, 175.

- (6) Kong, J.; Chapline, M. G.; Dai, H. J. *Adv. Mater.* **2001**, *13*, 1384.
(7) Bodzenta, J.; Burak, B.; Gacek, Z.; Jakubik, W. P.; Kochowski, S.; Urbanczyk, M. *Sens. Actuators, B* **2002**, *87*, 82.
(8) Offermans, P.; Tong, H. D.; van Rijn, C. J. M.; Merken, P.; Brongersma, S. H.; Crego-Calama, M. *Appl. Phys. Lett.* **2009**, *94*, 223110.
(9) For a nice review, please see: Christofides, C.; Mandelis, A. *J. Appl. Phys.* **1990**, *68*, R1.
(10) Chen, H.-I.; Chou, Y.-I.; Chu, C.-Y. *Sens. Actuators, B* **2002**, *85*, 10.
(11) Wang, C.; Mandelis, A.; Garcia, J. A. *Rev. Sci. Instrum.* **1999**, *70*, 4370.
(12) Sutapun, B.; Tabib-Azar, M.; Kazemi, A. *Sens. Actuators, B* **1999**, *60*, 27.
(13) Pundt, A. *Adv. Eng. Mater.* **2004**, *6*, 11.
(14) Lee, E.; Lee, J. M.; Koo, J. H.; Lee, W.; Lee, T. *Int. J. Hydrogen Energy* **2010**, *35*, 6984.
(15) Yang, F.; Taggart, D. K.; Penner, R. M. *Nano Lett.* **2009**, *9*, 2177.
(16) Favier, F.; Walter, E. C.; Zach, M. P.; Benter, T.; M. Penner, R. M. *Science* **2001**, *293*, 2227.
(17) Walter, E. C.; Favier, F.; Penner, R. M. *Anal. Chem.* **2002**, *74*, 1546.
(18) Jeon, K. J.; Jeun, M.; Lee, E.; Lee, J. M.; Lee, K. I.; von Allmen, P.; Lee, W. *Nanotechnology* **2009**, *19*, 495501.
(19) Jeon, K. J.; Lee, J. M.; Lee, E.; Lee, W. *Nanotechnology* **2009**, *20*, 135502.
(20) Yu, S. F.; Welp, U.; Hua, L. Z.; Rydh, A.; Kwok, W. K.; Wang, H. H. *Chem. Mater.* **2005**, *17*, 3445.
(21) Xu, T.; Zach, M. P.; Xiao, Z. L.; Rosenmann, D.; Welp, U.; Kwok, W. K.; Crabtree, G. W. *Appl. Phys. Lett.* **2005**, *86*, 203104.
(22) Khanuja, M.; Kala, S.; Mehta, B. R.; Kruis, F. E. *Nanotechnology* **2009**, *20*, 015502.
(23) Yang, F.; Taggart, D. K.; Penner, R. M. *Small* **2010**, *6*, 1422.
(24) Yang, F.; Kung, S.-C.; Cheng, M.; Hemminger, J. C.; Penner, R. M. *ACS Nano* **2010**, *4*, 5233.
(25) Menke, E. J.; Thompson, M. A.; Xiang, C.; Yang, L. C.; Penner, R. M. *Nat. Mater.* **2006**, *5*, 914.
(26) <http://www.whatman.com/PRODAnoporeInorganicMembranes.aspx>.
(27) Xiao, Z. L.; Han, C. Y.; Welp, U.; Wang, H. H.; Kwok, W. K.; Willing, G. A.; Hiller, J. M.; Cook, R. E.; Miller, D. J.; Crabtree, G. W. *Nano Lett.* **2002**, *2*, 1293, and references therein.
(28) Thomas, R. C.; Hughes, R. C. *J. Electrochem. Soc.* **1997**, *144*, 3245.
(29) Narehood, D. G.; Kishore, S.; Goto, H.; Adair, J. H.; Nelson, J. A.; Gutierrez, H. R.; Eklund, P. C. *Int. J. Hydrogen Energy* **2009**, *34*, 952.
(30) Eastman, J. A.; Thompson, L. J.; Kestel, B. J. *Phys. Rev. B* **1993**, *48*, 84.
(31) Hughes, R. C.; Schubert, W. K. *J. Appl. Phys.* **1992**, *71*, 542.